



The importance of rheology characterization in predicting turbulent pipe flow of generalized Newtonian fluids



J. Singh^a, M. Rudman^{a,*}, H.M. Blackburn^a, A. Chryss^b, L. Pullum^c, L.J.W. Graham^b

^a Department of Mechanical and Aerospace Engineering, Monash University, Vic 3800, Australia

^b CSIRO Minerals Resources Flagship, Clayton, Vic 3168, Australia

^c Private consultant, Olinda, Vic 3788, Australia

ARTICLE INFO

Article history:

Received 14 November 2015

Revised 16 February 2016

Accepted 23 March 2016

Available online 30 March 2016

Keywords:

Generalized Newtonian fluid

Turbulent pipe flow

Rheology characterisation

Direct numerical simulations (DNS)

ABSTRACT

Most Direct Numerical Simulation (DNS) of turbulent flow of generalized Newtonian (GN) fluids presented to date have shown significant discrepancy between experimental measurement and simulation. In addition to DNS, empirical correlations using different rheology models fitted to the same shear rheogram have also shown to give significantly different results. Important to note is that for turbulent flow predictions it is a common practice to use a shear rheogram which is measured at shear rates well below the values encountered in turbulent flows. This paper highlights the importance of obtaining high shear rate rheology in reducing these discrepancies. Further, it is shown that if high shear rate rheology is used in rheology characterisation, the choice of rheology model has little influence on the results. An important aside is that accurate prediction of laminar flow gives absolutely no confidence that a rheology model is acceptable in modelling the turbulent flow of the same fluid. From an analysis of instantaneous shear rates in the predicted turbulent flow field, the probability distribution of the non-dimensionalised shear rates in the near-wall region appears to collapse onto a universal curve. Based on this, we propose that the maximum shear rate required in rheology characterisation should be at least twice the shear rate corresponding to the mean wall shear stress.

© 2016 Elsevier B.V. All rights reserved.

1. Introduction

Many fluids in industrial applications and nature show non-Newtonian behaviour i.e. they do not show a uniform viscosity under isothermal conditions. Generalised Newtonian (GN) fluids are a class of non-Newtonian fluids for which the shear stress tensor $\boldsymbol{\tau}$ can be expressed as a product of a non-constant viscosity and the strain rate tensor:

$$\boldsymbol{\tau} = 2\mu(\dot{\gamma})\boldsymbol{S} \quad (1)$$

Here, $\dot{\gamma}$ is the second invariant of the strain rate tensor $\boldsymbol{S} = \frac{1}{2}[\nabla\boldsymbol{v} + (\nabla\boldsymbol{v})^T]$ determined as $\dot{\gamma} = \sqrt{(2\boldsymbol{S} : \boldsymbol{S})}$ and μ is a scalar viscosity usually called an effective or apparent viscosity. The GN assumption assumes an instantaneous response of the fluid to the applied shear stress and therefore, the viscosity of a GN fluid can be expressed as a function of shear rate $\dot{\gamma}$ as in Eq. 1. Note that the effective viscosity of a GN fluid can also depend on temperature, but we do not consider the effect of temperature in the current study. In practice, the effective or apparent viscosity of a GN fluid

is determined by dividing the shear stress measured in a rheometer by the shear rate at which the stress is measured. These measurements are performed in a uni-directional flow in a rheometer. Fine particle suspensions, sewage sludges, molten lava, some polymer solutions, some bodily fluids and paints are examples of fluids that are well approximated by the GN assumption. Although the apparent viscosity of these fluids is often very high, industrially relevant flows can be turbulent at sufficiently high flow rates or in pipes with sufficiently large diameters. Despite their wide applications, there have been only a few studies dedicated to the fundamental understanding of turbulent flow of GN fluids, the majority of which have been experimental [1–6] with the primary objective often to derive a general correlation for the friction factor.

Unlike Newtonian fluids where the kinematic viscosity can be measured very accurately, non-Newtonian fluids are far more difficult to characterise. Despite this, the assumption of GN behaviour as a constitutive model appears to work well for a range of fluids. However, the constitutive equation relating the shear stress and shear rate is usually determined by fitting a particular mathematical rheology model to the experimental measured shear rheogram. There are many rheology models available for GN fluids [7,8], but the Herschel–Bulkley [9] and the Hallbom rheology models

* Corresponding author. Tel.: +61409033037.

E-mail address: murray.rudman@monash.edu (M. Rudman).

[10] have been found to represent the rheology of fluids such as mining and waste water slurries quite well [10–12]. The Herschel–Bulkley model defines the effective viscosity as:

$$\mu = \tau_y / \dot{\gamma} + K(\dot{\gamma})^{n-1} \quad (2)$$

Here, the yield stress τ_y , consistency K and flow index n are the model parameters. This model reduces to the power-law rheology model giving $\mu = K(\dot{\gamma})^{n-1}$ when $\tau_y = 0$ and the Bingham model $\mu = \tau_y / \dot{\gamma} + K$ when $n = 1$, both of which are commonly used in application. Unlike the Herschel–Bulkley model which has no theoretical basis [10], the Hallbom rheology model (Eq. 3) is derived by considering the behaviour of solid particles in homogeneous shear-thinning mineral suspensions and relates the viscosity and shear rate via the following equation:

$$\mu^k = (\tau_0 / \dot{\gamma})^k + (\mu_\infty)^k \quad (3)$$

In this equation the model parameters are known as the yield stress τ_0 , the infinite shear viscosity μ_∞ and the scaling factor k . The benefit of the Hallbom model in approximating (for example) a fine particle suspension is that as $\dot{\gamma} \rightarrow \infty$, the carrier fluid rheology is recovered, unlike the Herschel–Bulkley model in which the predicted viscosity drops below that of the carrier fluid. This is not physically possible.

Rheograms used for determining rheology model parameters in industrial application are typically measured over shear rates that would rarely exceed 500 s^{-1} (and often significantly less). This range is well below the shear rates that could be encountered in turbulent flow. Another way of determining the model parameters for the rheology models discussed here is via the use of analytical expressions that relate the bulk velocity (volumetric flow rate per unit cross-sectional area) and pressure gradient under laminar flow conditions to the model parameters [7,8]. These relationships can be (and often are) used for determining rheology parameters from the measured laminar flow curve (i.e. flow rate versus pressure drop), often in a small scale laboratory pipe loop. The shear rate range over which laminar flow is appropriate will depend on the fluid and pipe diameter. For laboratory experiments it is typically less than 300 s^{-1} and sometimes much smaller. It has been shown that constitutive equations based on different rheology models determined from the same laminar pipe data when used with theoretical or empirical correlations for determining the friction factor give barely distinguishable results in the laminar region as expected. However, the discrepancy in the turbulent regime can be as large as 50% [12,13]. Regardless, it is a common practice in hydraulic conveying to use such measurements.

Numerical techniques such as Reynolds Averaged Navier–Stokes (RANS), large eddy simulation (LES) and direct numerical simulations (DNS) require a constitutive equation for estimating viscosity. Although simulation of turbulent flow of GN fluids using these numerical techniques, particularly DNS, show encouraging outcomes [14–16], the most fundamental flow prediction (flow rate versus pressure drop, or equivalently friction factor) is usually in error. In DNS of pseudo-plastic fluids, Rudman *et al.* [14] found that for a given pressure gradient the bulk velocity predicted by DNS was 25% lower than the experimental value. Given that the same code at a similar resolution was able to predict the turbulent flow of a Newtonian fluid to within a few percent, this level of error is unacceptable. The discrepancy between DNS and experiments could be due to the following factors:

1. Inaccurate experimental measurements;
2. Poor choice of simulation method and parameters in terms of method accuracy, simulation resolution, computational domain length and time duration over which results are averaged;
3. The rheology measurements and/or data fitting;
4. The assumption of a GN rheology model.

Given that the experimental techniques used for the pipe flow measurements reported in Rudman *et al.* are standard and were validated against well characterised water data, experimental error is believed to be far smaller than the observed discrepancy. Thus, the first point is unlikely to be the cause. A spectral element–Fourier method which is exponentially convergent [17] was used in that study and domain length and mesh convergence were ensured, therefore, the second point is also unlikely to be the cause. In their simulations, Rudman *et al.* observed that the instantaneous, local shear rates spanned many orders of magnitude and were predicted to be significantly higher than those values used in the rheological characterisation. They suggested that the extrapolation of the shear rheogram for estimating viscosity beyond the range of shear rate where it was measured lead to the observed discrepancy between simulation and experiment. Thus the third point remains a possibility. The assumption that a GN model is appropriate is a difficult one to demonstrate conclusively. Although it remains a possibility that the GN assumption is not valid, we do not consider this as an alternative here. We agree with the argument in Rudman *et al.*, and later demonstrate, that the majority of the discrepancy arises due to poor rheology characterisation at high shear rates. It is worth noting that for turbulent flow predictions using empirical correlations (for example Dodge & Metzner [2] and Wilson & Thomas [18]), the importance of high shear rate rheology has also been advocated by other researchers [2,7,19]. Shook & Roco [19] suggest that for turbulent flow predictions, the shear rheogram used in rheology characterisation should be measured to shear rates at least as high as those corresponding to the mean wall shear stress τ_w .

The objectives of the present study are three-fold. First we aim to show that shear rheograms determined using traditional approaches such as laminar pipe flow curves or rheometry measured at low shear rates, when extrapolated to shear rates relevant to turbulent flows can deviate significantly from the actual rheology. By including the high shear rate rheology of the fluid in rheological characterisation, discrepancies between experiments and predictions using DNS or empirical turbulent flow correlations can be significantly reduced. Second, if an appropriate range of shear rates is considered in the rheology characterisation, the choice of the rheology model has a very small effect on turbulent flow predictions of DNS or empirical correlations. The third objective of this study is to define a criterion for the maximum shear rate (and shear stress) to use in rheology characterisation in order for DNS to produce good results. In the process of determining this we analyse the shear rate distribution in turbulent pipe flow field for the first time. The results suggest that in the near-wall region, the probability distribution of non-dimensionlised instantaneous shear rate collapses to a universal distribution for different models, fluids and Reynolds numbers. Based on this observation we propose that for turbulent flow predictions of shear-thinning fluids, the rheology characterisation should use the rheogram measured at least up to twice the mean wall shear stress.

2. Pipe flow measurements

The pipe flow test apparatus is shown schematically in Fig. 1. It comprises a 14 m pipe loop (≈ 300 diameters) with an internal diameter of 44.5 mm. A 400 litre agitated tank supplies a Warman $2 \times 1\frac{1}{2}$ AH variable speed pump for circulating fluids around the loop. The pressure gradients in both the upper and lower horizontal lines are measured using differential pressure (DP) cells spanning straight sections of pipe. The volumetric flow rate is monitored via a magnetic flow-meter. The rig instrumentation is data logged using a stand-alone LabVIEW application allowing the normal transport flow characteristics to be obtained in real time. In order to test the instrumentation a water-only flow curve was

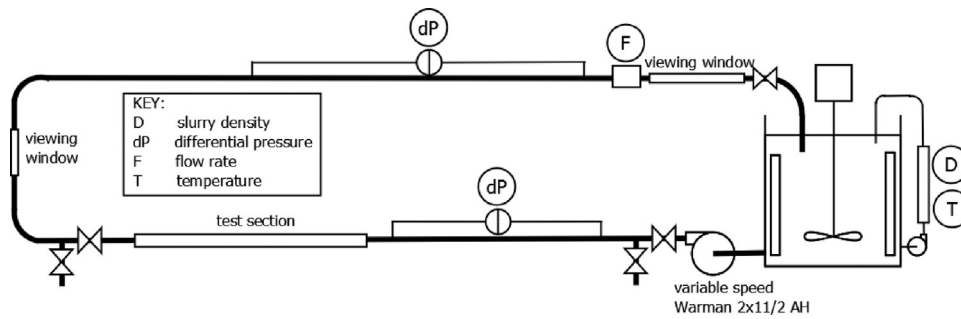


Fig. 1. Schematic of pipe rig.

obtained and compared against the established values for a hydraulically smooth pipe (based on pipe Reynolds number and Darcy–Weisbach friction factor). The agreement was within expected variations; $\pm 5\%$ at a bulk velocity $U_b = 0.2 \text{ m s}^{-1}$ and $\pm 2\%$ at $U_b = 3.0 \text{ m s}^{-1}$. The majority of the measurement error arises from measuring at the low end of the pressure sensor. This implies that more accurate readings are probable for the Carbopol fluid under investigation, as the Carbopol fluid requires much higher pressure gradients than water.

For the data used in this study, 300 litres of Carbopol 980 solution was made and allowed to stabilise. The nominal concentration of the solution was 0.075 wt% and the solution was neutralised using sodium hydroxide to a pH between 6.5 and 7. The tests required a series of steady flow rate conditions to be established and pressure drop on both legs to be recorded and time-averaged. The pressure drop measurements were taken for flow rates from the laminar region to the turbulent. They were sampled at 0.5 Hz over a period of 300 s and time averaged. Spectral analysis was conducted on the data and no significant frequencies were detected, ensuring that the pressure readings are not affected by any unintended flow phenomena. The DP cells were 2 m apart and had an accuracy of 0.15% of full scale deflection, with a further allowance of 0.1% for ambient vibration effects. This equates to an uncertainty in pressure drop readings of $\pm 7.5 \text{ Pa m}^{-1}$. For a measured pressure gradient of 2500 Pa m^{-1} this corresponds to an error of 0.3%. The flow meter used had an accuracy of 0.25% which corresponds to an uncertainty of 0.007 m s^{-1} at a bulk velocity $U_b = 2.9 \text{ m s}^{-1}$. The temperature of the fluid in the pipe loop could not be controlled but was monitored via a Platinum Resistance Thermometer (PRT) inserted in the stream outside of the pressure measurement zones and also in the tank. The PRT is able to measure reliably to $\pm 0.1 \text{ }^\circ\text{C}$ and a maximum variation of $\pm 0.2 \text{ }^\circ\text{C}$ was recorded in the course of a single run. Any inaccuracy in the measured fluid density is predominantly due to the temperature change. The fluid behaves similarly to water in this regard and the uncertainty in density is therefore less than 0.01%.

3. Rheology measurements and characterisation

3.1. Measurement

A wide range of shear rates is covered in the rheology measurements by using two different measurement geometries; a concentric cylinder and a parallel plate (see Table 1). Using different geometries also provides a mean of confirming data where the measurements overlap. A Haake Rheostress RS1 rheometer was used throughout and temperature control was maintained via a recirculating water bath, with test temperatures matched to those in the pipe flow measurements (see Section 2) within $\pm 0.1^\circ\text{C}$. The concentric cylinder geometry was used to measure the rheology in low to medium shear rate region (see Table 1). The larger surface area

Table 1

Details of the geometries used in the rheometry and corresponding shear rate range.

Geometry	Dimensions	Shear-rate range
Concentric cylinder	Inner-Cylinder dia.= 38 mm, Outer-Cylinder dia.= 41 mm	0.01 – 100 s^{-1}
Parallel plate	Plate-dia.= 60 mm, gap=0.2 mm	10 – 15000 s^{-1}

of this geometry provided shear stress measurements that were 2.9 times more sensitive than the parallel plate geometry. The upper range of the measurements in the concentric cylinder geometry was limited due to the inaccuracies caused by the onset of Taylor-Couette eddies, a secondary flow effect at high shear rates [20]. In the unaffected region the correct shear rate (allowing for the non-Newtonian fluid effect) was obtained by using an integration approach for the Couette inverse problem [21]. This method is generally more successful than a differential approach due to the inevitable noise present in real data. For the measurements in the medium to high shear rate region, a parallel plate geometry was used. As high shear rate rheometry necessitate small measurement gaps the alignment of our parallel plate geometry was tested using a camera with a macroscopic lens calibrated against a 0.1 mm graticule. The rheometer gap measurement consistently underestimated the distance in the order of 0.01 mm when compared to the optical technique. This would produce an error of the order of 5% with the 0.2 mm gap used and the shear rate was recalculated accordingly. In this geometry, the calculation of the rim shear stress corrected for non-Newtonian fluids required the differentiation of measured instrument torque as a function of shear rate at the rim [22]. Duplicate results from each geometry, after any necessary corrections, were combined and averaged in the overlapping shear rate regions.

3.2. Characterisation

To address the aims of the paper, a number of different rheology characterisations are performed on the measured data. The model parameters of these characterisations are shown in Table 2 and the corresponding shear rheograms for the full shear rate range (0.01 to 15 000 s^{-1}) are plotted in linear and log coordinates in Fig. 2. We use the term ‘model’ in two different contexts below. In the first, ‘model’ type refers to the mathematical form of the rheological model we fit to (power-law, Herschel–Bulkley etc.). In the second, ‘model’ means the mathematical form plus the fitted parameters that describe the best fit to the data. The meaning should be clear from the usage. The curve fitting exercise to determine the rheology parameters from the measured data is carried out using the `lsqcurvefit` function in MATLAB which determines a least-square fit to a non-linear data set.

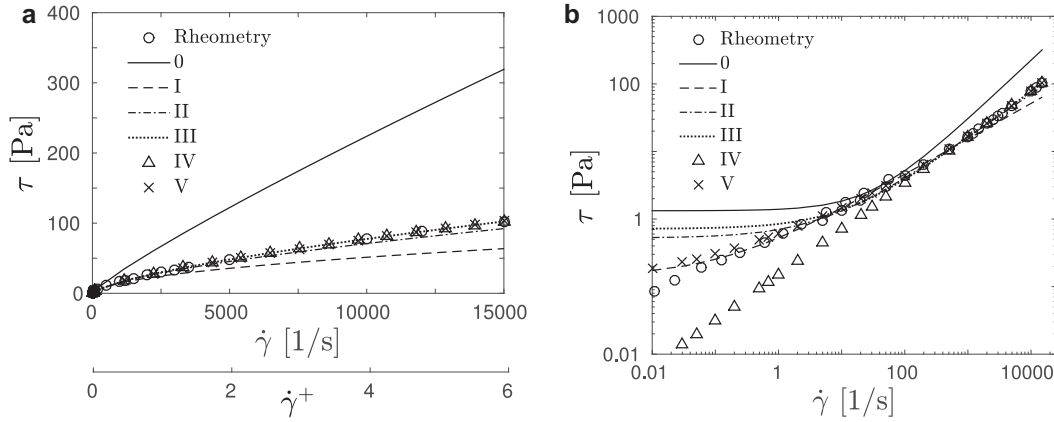


Fig. 2. Shear rheograms for different rheology models plotted in (a) linear and (b) log-log scales. Here $\dot{\gamma}^+ = \dot{\gamma}/(u_\tau^2/\nu_w)$ is the shear rate expressed in wall units. Low shear rate models *0* and *I* show large deviation from the measured rheology at high shear rates whereas high shear rate models *II–V* deviate from each other at very low shear rates.

Table 2

Rheology models determined using the laminar pipe flow curve and the measured shear rheogram with differing shear rate ranges. The first column is the rheology identifier, and the second column specifies what data was used in determining the model parameters.

Herschel–Bulkley		τ_y (Pa)	K (Pa.s ⁻ⁿ)	n
0	laminar pipe flow data	1.33	0.067	0.88
I	[0.01, 500] s ⁻¹	0.14	0.389	0.53
II	[0.01, 5 000] s ⁻¹	0.52	0.177	0.65
III	[0.01, 15 000] s ⁻¹	0.72	0.129	0.69
Power law			K (Pa.s ⁻ⁿ)	n
IV	[0.01, 15 000] s ⁻¹	–	0.15	0.68
Hallbom		τ_0 (Pa)	μ_∞^k (Pa.s ^{-k})	k
V	[0.01, 15 000] s ⁻¹	0.0526	0.311	0.169

Model 0

In rheology model *0*, the Herschel–Bulkley model is fitted to the laminar pipe flow curve (see Section 2) using the analytical expression given in Eq. 4.

$$U_b = nR \left(\frac{\tau_w}{K} \right)^{1/n} (1 - \phi)^{n+1/n} \left\{ \frac{(1 - \phi)^2}{3n + 1} + \frac{2\phi(1 - \phi)}{2n + 1} + \frac{\phi^2}{n + 1} \right\} \quad (4)$$

Here, $\phi = \tau_y/\tau_w$ and τ_w is the mean wall shear stress calculated from the axial pressure gradient ($\tau_w = (D/4)dp/dz$). As seen in Fig. 2a and b, the shear rheogram of fit *0* deviates significantly from the measured data at both high and low shear rates. Worth noting in this regard is that the maximum shear rate (estimated from the analytical velocity profile) is ≈ 500 s⁻¹, however, rheology fit *0* fails to represent the rheology of the fluid accurately for shear rates $\dot{\gamma} > 100$ s⁻¹.

Models I–III

The rheogram obtained using the rheology measurement techniques described in Section 3.1 is used to fit the Herschel–Bulkley model over three different shear rate ranges to give models *I*, *II* and *III*, each with an increasing upper bound of maximum shear rate, (500 s⁻¹, 5000 s⁻¹ and 15000 s⁻¹) and all with the lower bound of 0.01 s⁻¹.

The maximum shear rate considered in model *I* (500 s⁻¹) is typical of an industrial laboratory measurements and similar to the maximum implied in model *0*. As seen in Fig. 2a, model *I* clearly deviates below the measured rheology at shear rates $\dot{\gamma} > 1000$ s⁻¹ indicating that the viscosity estimates using this rheology fit will be in error at high shear rates.

Rheology model *II* used the measured shear rheogram in the range of shear rate $\dot{\gamma} = 0.01 - 5000$ s⁻¹. This maximum shear rate is chosen based on an analysis of our DNS results where we observed that the instantaneous shear rates in the flow field were usually less than 5000 s⁻¹ (see Section 5.3). This model deviates from the measured data for low shear ($\dot{\gamma} < 10$ s⁻¹) and a little for higher shear ($\dot{\gamma} > 5000$ s⁻¹).

Model *III* used the shear rheogram over the full range of measured shear rate data, i.e. $\dot{\gamma} = 0.01 - 15000$ s⁻¹.

Models IV and V

Model *IV* is based on the power-law model and model *V* is based on the Hallbom model. Both use data over the full range of measured shear rate, $\dot{\gamma} = 0.01 - 15000$ s⁻¹. We observed that the shear rheogram of the Hallbom model is very sensitive to the parameter μ_∞ (see Eq. 3) which is of order 10^{-5} Pa s^{-k}. Hence we choose μ_∞^k as the fitted parameter. As seen in Fig. 2a and b, the rheology predictions of models *IV* and *V* are good at high shear rates, although the power-law model deviates below the measurements for $\dot{\gamma} < 100$ s⁻¹. The Hallbom model agrees well for all shear rates $\dot{\gamma} > 1.0$ s⁻¹.

Summary

Except at very low shear rates (or 100 s⁻¹ in the case of model *IV*), the rheograms of models *II–V* agree well with the measured data. Deviation, especially at quite low shear rates, highlights the difficulties associated with finding a universal model fit which can represent the rheology of a fluid over a very wide range of shear rates. The Hallbom model comes closest to fulfilling the condition of universality. For a given rheology model, the model parameters vary with the shear rate range used in rheology characterisation (see *I–III* in Table 2 for the Herschel–Bulkley fits). This highlights the fact that while a rheology model aims to capture the essence of the fluid rheology, the parameters determined from the curve fitting exercise usually have no direct physical basis in themselves.

It is worth noting that at lower shear rates, model fits to the rheometric data (models *I–V*) deviate significantly below model *0* (the rheology fit determined from the laminar pipe flow curve). Given that model *0* predicts the laminar flow behaviour very well, it is clear that laminar flow rate predictions using any of models *I–V* will likely be in error. An important corollary of this is that accurate prediction of laminar flow behaviour is no indicator of model performance in the turbulent flow through the same pipe and that such agreement cannot be used as validation data for turbulent flow prediction. Indeed, poor prediction in laminar flow does not automatically invalidate the accuracy of a model in turbulent flow, in direct contradiction to usually accepted practice with Newtonian fluids. As a final comment, rheology measurements at

low shear rates are difficult and most likely to be error-prone in normal measurement situations. We will later demonstrate that inadequacy of low shear rate rheology does not affect turbulent flow predictions significantly.

A note on visco-elasticity

Peixinho et al. (2005) [23] measured the rheology of a 0.2 wt% Carbopol solution and observed visco-elastic effects for shear stresses greater than approximately 110 Pa. The shear stress value for which visco-elasticity becomes important will increase with decreasing Carbopol concentration. Because the concentration used here is approximately 0.075 wt%, visco-elastic effects will not become noticeable for us until the shear stresses becomes significantly higher than 110 Pa. Even at the highest shear rates we measure (15 000 s⁻¹), the shear stress does not exceed 90 Pa. Thus our 0.075 wt% Carbopol solution can be confidently modelled as an inelastic fluid.

4. Computational methodology

4.1. Numerical method

A nodal spectral element-Fourier DNS code [15,17] is used to solve the following governing equations written for the flow of an incompressible GN fluid.

$$\partial \mathbf{v} / \partial t + \mathbf{v} \cdot \nabla \mathbf{v} = -\nabla p + \nabla \boldsymbol{\tau} + \mathbf{f}, \quad \text{with} \quad \nabla \cdot \mathbf{v} = 0. \quad (5)$$

Here \mathbf{v} is the velocity vector, p is the modified or kinematic pressure i.e. pressure divided by a constant density, $\boldsymbol{\tau}$ is the shear stress tensor given by Eq. 1 where the viscosity μ is calculated using the rheology model. In Eq. 5, \mathbf{f} is the constant body force per unit mass, which is set equal to the pressure gradient divided by density. The code uses Fourier expansions in the axial direction and thus strictly enforces axial periodicity. Simulations were run until the calculated total wall shear stress is statistically converged, usually it fluctuates a little about a mean value. Once this dynamic steady state is reached, mean fields and turbulence statistics are collected for approximately twenty domain wash-through times.

4.2. Non-dimensional units

Results are non-dimensionalised in the standard manner. The mean wall shear stress is related to the pressure gradient via

$$\tau_w = \frac{D}{4} \frac{\partial P}{\partial z}. \quad (6)$$

Here, D is the diameter of the pipe. The mean axial velocity U is expressed in wall units as $U^+ = U/u_\tau$ where $u_\tau^2 = \tau_w/\rho$. Distance from the wall is expressed in wall units as $y^+ = (R-r)u_\tau/\nu_w$ where ν_w is the mean wall viscosity, r is the radial distance from the centre of the pipe and R is the radius of the pipe. The mean wall viscosity is calculated directly from the pressure gradient via Eq. 6 and the rheology model. For the Herschel-Bulkley model ν_w is determined from the mean wall shear stress as:

$$\nu_w = \frac{K^{1/n}}{\rho} \frac{\tau_w}{(\tau_w - \tau_y)^{1/n}}. \quad (7)$$

For the power-law rheology model ν_w is easily recovered by setting $\tau_y = 0$ in Eq. 7. For the Hallbom rheology model, ν_w is calculated using the following expression [8]:

$$\nu_w = \frac{\mu_\infty}{\rho(1 - Z^k)^{1/k}}, \quad \text{with} \quad Z = \frac{\tau_0}{\tau_w} \quad (8)$$

The non-dimensional shear rate is expressed in wall units as $\dot{\gamma}^+ = \dot{\gamma}/(u_\tau^2/\nu_w)$.

Because viscosity is not uniform in GN fluids, the definition of a suitable Reynolds number is not immediately clear. Here we will

use the mean wall viscosity ν_w as the viscosity scale and define a generalized Reynolds number Re_G and a friction Reynolds number Re_τ using the bulk velocity U_b and friction velocity u_τ . These Reynolds numbers are:

$$Re_G = \frac{U_b D}{\nu_w}, \quad \text{and} \quad Re_\tau = \frac{u_\tau D}{\nu_w}. \quad (9)$$

4.3. Resolution and domain independence

A grid resolution and domain independence study using rheology model III was performed to ensure that the mean flow profiles and turbulence statistics do not change with mesh refinement or domain length. The final mesh had 16,500 grid points in the pipe cross-section with 288 Fourier planes in the axial direction giving 5.6 M node points. The near-wall mesh spacings expressed in wall units (defined above) are $\Delta r^+ = 1.3$, $r\Delta\theta^+ = 7$ and $\Delta z^+ = 25$ which correspond well to typical rules-of-thumb for wall resolving DNS [24].

4.4. Wilson-Thomas correlation for friction factor

There are several empirical correlations commonly used for predicting the friction factor in turbulent flow of GN fluids [18,25–27]. Our aim here is to understand if the predictive capability of such correlations is also improved by the use of high shear rate rheometry. We choose one correlation, the Wilson-Thomas correlation [18], because it is easily expressed for the three rheology models we consider. This correlation relates the bulk velocity U_b and friction velocity $u_\tau = \tau_w/\rho$ via:

$$U_b = 2.5u_\tau \ln \left(\frac{Du_\tau}{\nu_w} \right) + u_\tau (11.6(\alpha - 1) - 2.5 \ln(\alpha)). \quad (10)$$

Here α is the ratio of the area of rheograms of the non-Newtonian and Newtonian fluids up to the mean wall shear rate $\dot{\gamma}_w$. For a given rheology model, the area under the rheogram is given by

$$A = \int_{\dot{\gamma}=0}^{\dot{\gamma}_w} \mu(\dot{\gamma}) \dot{\gamma} d\dot{\gamma} \quad (11)$$

Solving the above integration for a Newtonian fluid gives $A = \frac{1}{2} \dot{\gamma}_w \tau_w$ and with the Herschel-Bulkley rheology model this gives $A = \dot{\gamma}_w (\tau_w + n\tau_y)/(n+1)$. Hence, the area ratio for a Herschel-Bulkley fluid can be written as $\alpha = (2/(n+1))(1 + n\tau_y/\tau_w)$. For the Hallbom rheology model a general expression for calculating α is written as [8]:

$$\alpha = \frac{2}{\dot{\gamma}_w} \int_{\dot{\gamma}=0}^{\dot{\gamma}_w} \left[\left(\frac{\tau_0}{\tau_w} \right)^k + \left\{ 1 - \left(\frac{\tau_0}{\tau_w} \right)^k \right\} \left(\frac{\dot{\gamma}}{\dot{\gamma}_w} \right)^k \right]^{1/k} d\dot{\gamma} \quad (12)$$

For integer values of $1/k$ the above integration can be solved directly, however, for non-integer values of $1/k$, this integration must be carried out numerically.

5. Results and discussion

We split the comparison of DNS and experimental results into two main parts. First is the effect that shear rate range used in the rheology characterisation has on the turbulent flow predictions. In the second, the effect that the rheology model type has on the comparison is considered, given the models are based on identical shear rate data.

The measured experimental flow data is shown in Fig. 3. There are two points in the transitional regime and two in the turbulent, and below we consider results primarily at the highest flow velocity, 2.90(± 0.01) m s⁻¹, with some additional comparisons at the next highest velocity, 2.70(± 0.01) m s⁻¹.

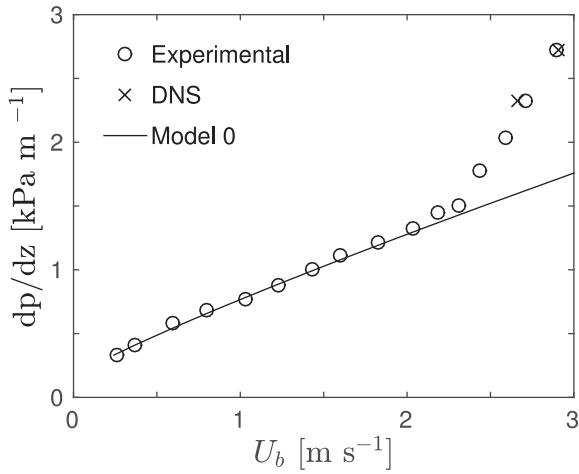


Fig. 3. Pressure gradient versus bulk velocity measured in (o) experiments and (x) predicted by DNS with rheology model *III*. The solid line is the laminar flow curve of model 0. The critical velocity of transition of flow from laminar to turbulent (identified as the point where the laminar flow curve deviates from the experimental data) is $\approx 2.3 \text{ m s}^{-1}$. DNS are run for the two highest bulk velocities measured in experiments i.e. $V = 2.70 \text{ m s}^{-1}$ and $V = 2.90 \text{ m s}^{-1}$.

5.1. Effect of the shear rate range in rheology characterisation

To consider the effect of shear rate range, we use models 0–*III* which are based on the Herschel–Bulkley rheology model but use different shear rate ranges. DNS are run using these mod-

Table 3

Flow Reynolds number Re_G , Re_τ and the error in bulk velocity predictions using DNS and the Wilson–Thomas correlation (Eq. 10) at $dp/dz = 2.72 \text{ kPa m}^{-1}$.

Rheology	Re_τ	Re_G	Error in DNS (%)	Error in Wilson–Thomas (Eq. 10) (%)
0	241	3500	–13	–12
I	887	16,000	8.3	19
II	666	11,300	1.2	10
III	633	10,600	0.3	7
IV	627	10,516	0.4	7.3
V	638	10,844	1.6	9.4

els for an axial pressure gradient $dp/dz = 2.72(\pm 7) \text{ kPa m}^{-1}$. The measured bulk velocity in experiments at this pressure gradient was $2.90(\pm 0.01) \text{ m s}^{-1}$. Predictions of the bulk velocity U_b using DNS and the Wilson–Thomas correlation are compared against the experimental value in Table 3. Given that rheology models 0 and *I* showed poor agreement with the measured rheology data, the large errors in predicted U_b with these models is expected (see Table 3). DNS underpredicts the bulk velocity U_b by 13% using model 0 whereas it overpredicts it by approximately 8% using model *I*. With high shear models *II* and *III*, DNS prediction of U_b comes very close to the experimental value (within 2%). Similar trends (although different magnitudes) are also seen in the prediction of U_b using the Wilson–Thomas correlation (Eq. 10) with the error decreasing to 7% with fit *III* compared to 19% with fit *I*.

Mean flow profiles are presented in Fig. 4a and b. For ease of discussion, we divide the flow into a wall-region ($y^+ < 10$), buffer-layer ($10 < y^+ < 30$), log-layer ($30 < y^+ < 200$) and core ($y^+ >$

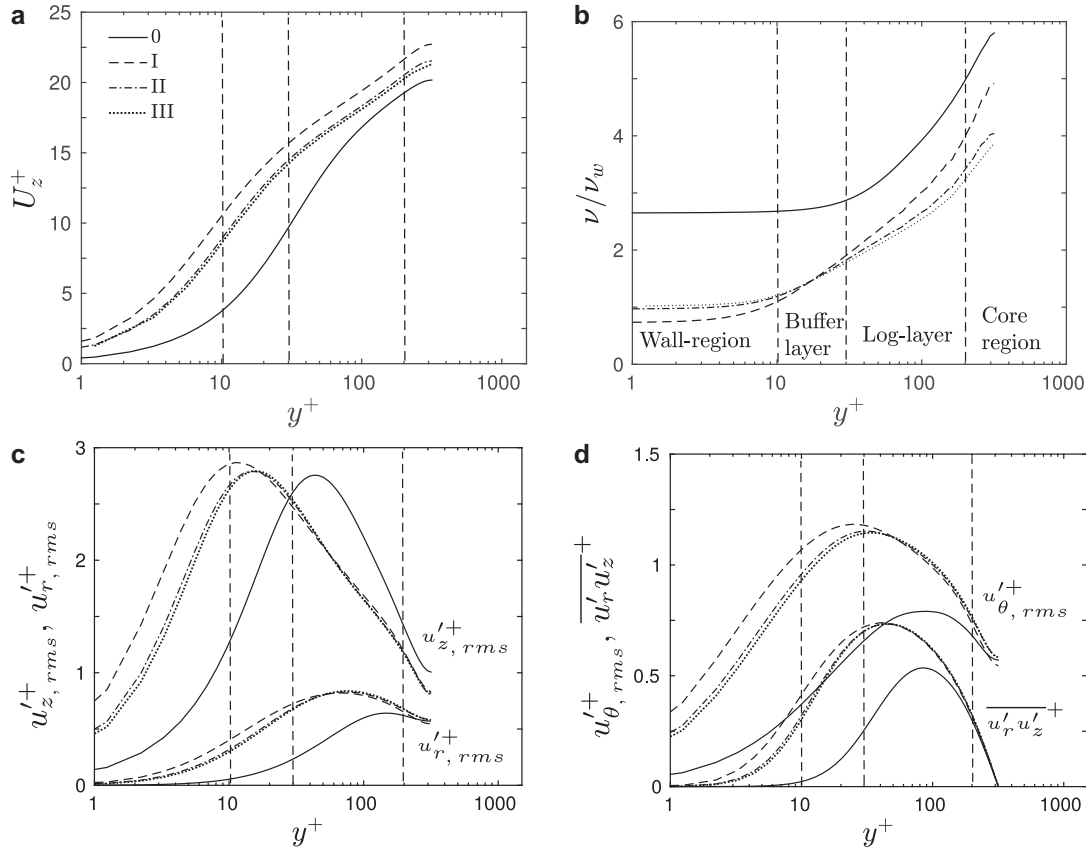


Fig. 4. The effect of shear rate range used in rheology characterisation in predicting flow at $dp/dz = 2.72 \text{ kPa m}^{-1}$. All are Herschel–Bulkley models, with model 0 determined from the laminar pipe flow data and models *I*–*III* determined from increasing range of shear rate. Profiles of (a) mean axial velocity (b) mean viscosity and (c,d) the turbulence statistics. Division of the flow region based on the distance from the wall y^+ is shown in (b). The mean wall viscosity ν_w of fit *III* is used in calculating y^+ . Profiles of low shear rate models 0 and *I* can be seen deviating from those of high shear rate models *II* and *III* which agree well with each other except the mean viscosity profiles where a small offset between the profiles of models *II* and *III* can be seen in log-layer and core-region.

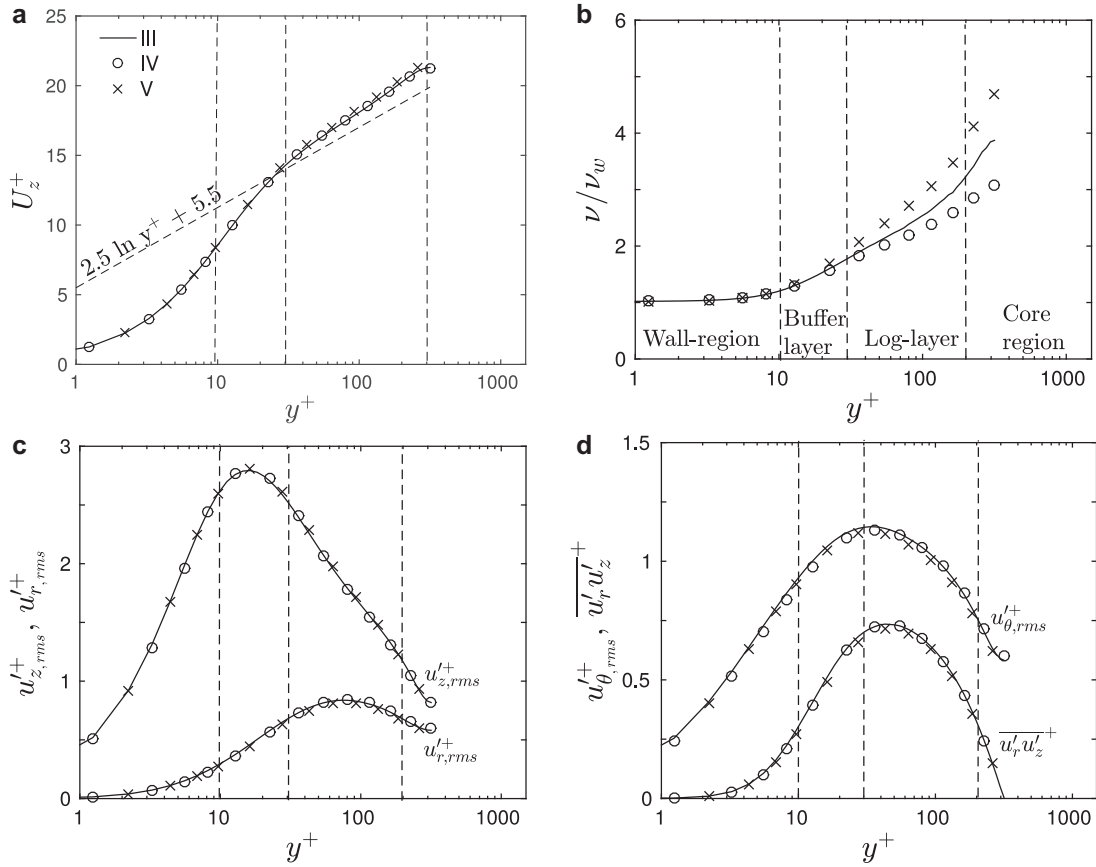


Fig. 5. The effect of rheology model type on mean flow profiles. Model III is Herschel–Bulkley, model IV is power–law and model V is a Hallbom model. Profiles of (a) mean axial velocity (b) mean viscosity and (c,d) turbulence statistics of different high shear rate models III–V at $dp/dz = 2.72 \text{ kPa m}^{-1}$. The dashed line in (a) shows the classical Newtonian log law $U_z^+ = 2.5 \ln y^+ + 5.5$. The mean wall viscosity ν_w of model III is used to calculate y^+ . Except mean viscosity, profiles of all rheology models agree very closely with each other.

200). Note that at such low Reynolds number ($Re_G \approx 10\,000$) splitting the flow into regions based on these numbers is somewhat arbitrary, however the results will later vindicate this choice. The general picture for models I–III is similar with a linear near-wall layer, a small log-like region and core that lifts very slightly above the log profile, not easily seen in the figure.

Results from model 0 have the hallmark of being a transitional flow without an obvious log-like region in the profile. This is in agreement with the higher viscosity predicted by this model at high shear rates. Consistent with the predictions of U_b , the mean axial velocity profiles of models II and III are close to each other and the profile of model I deviates (Fig. 4a). Note that ν_w of model III is used in non-dimensionalisation which ensures that if the profiles collapse in wall units, they will collapse in the physical units too. Hence, the results of different rheology models can be compared directly. If we scale the profiles, particularly of the mean axial velocity and viscosity, of different rheology models with their respective ν_w , the profiles would collapse in the wall region making it difficult to interpret the results.

The mean viscosity profile for each case is nearly uniform in the wall layer and appears to have a log-like region in part of the y^+ region corresponding to the velocity log-region, but then increases significantly toward the core of the flow. Rheograms of models II and III deviated from each other at low shear rates ($\dot{\gamma} < 50 \text{ s}^{-1}$) (Fig. 2b) and this is reflected in the mean viscosity profiles in the log-layer and core. Note that this difference in mean viscosity does not affect the mean axial velocity profile to any notable extent.

Understanding the relationship between different rheology models and the resulting predicted velocity profile (and value of U_b) is straightforward. In a pipe flow, the total mean shear stress τ at any radial location r is given by

$$\tau = \tau_w \left(\frac{r}{R} \right). \tag{13}$$

In the wall region specifically, where the velocity fluctuations decay to zero, almost all of the stress is due to the mean viscosity. As seen from Fig. 4b the mean viscosity is nearly uniform in the wall layer. Together these two considerations allow us to write,

$$\tau_w \left(\frac{r}{R} \right) \approx \rho \nu_w \frac{\partial U_z}{\partial r} \tag{14}$$

or

$$\frac{\partial U_z}{\partial r} \approx \frac{\tau_w}{\rho \nu_w} \left(\frac{r}{R} \right) = \dot{\gamma}_w \left(\frac{r}{R} \right). \tag{15}$$

For a given τ_w , the viscosity profile that predicts a higher viscosity at a given shear will also result in a lower wall shear rate. From Eq. 15, lower shear rate equates to a lower increase in velocity with distance from the wall, at least within the wall region. Beyond the wall layer, the mean viscous shear stress decreases (and the viscosity increases) and differences in mean shear play less of a role in influencing the velocity profile and bulk velocity. The key influence occurs in the near-wall region. Thus overestimation of the viscosity by the rheology model will result in underestimation of the mean axial velocity, as seen for model 0 in Fig. 4a. Similarly, underestimation of viscosity will result in overestimation of

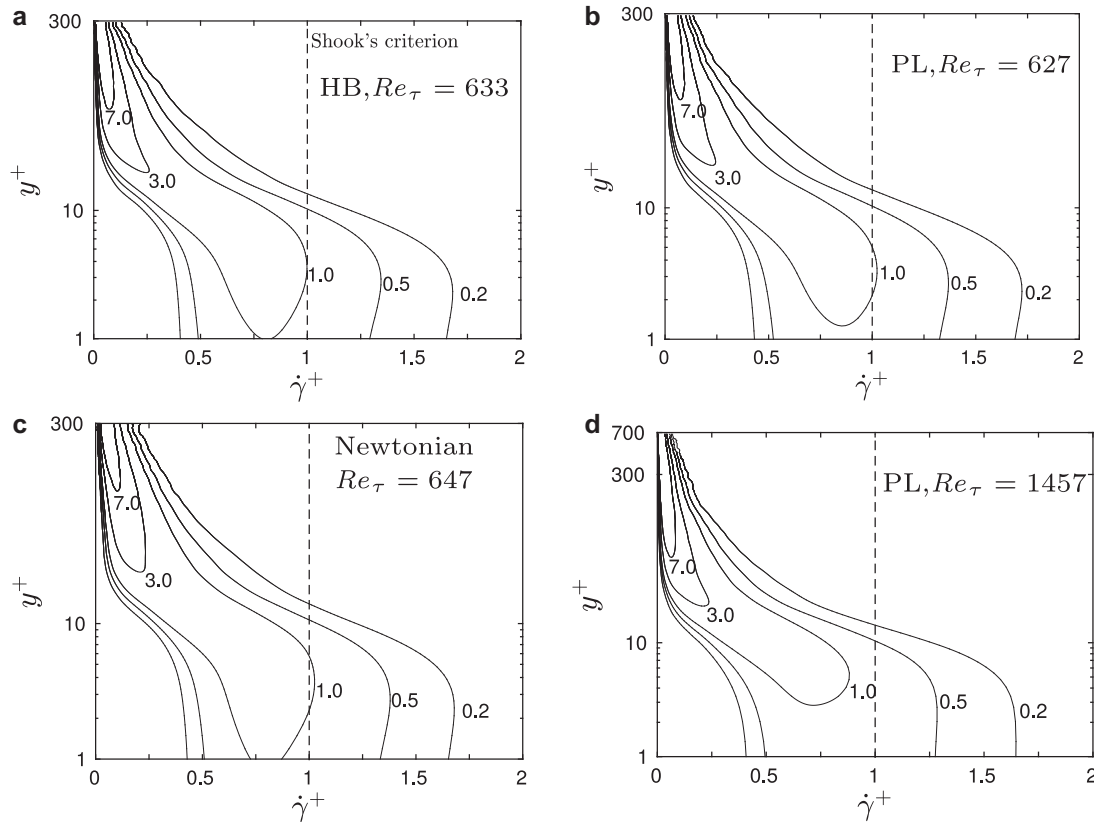


Fig. 6. Distribution of the conditional probability $p(\dot{\gamma}^+|y^+)$ of a fluid with (a) Herschel–Bulkley rheology *III* at $Re_\tau = 633$ (b) power–law rheology *IV* at $Re_\tau = 627$ (c) Newtonian rheology at $Re_\tau = 647$ and (d) the power–law rheology at $Re_\tau = 1457$. Contours are of % probability. The spread of the probability distribution of instantaneous shear rate near the wall when plotted in wall units is almost independent of the rheology and Re_τ .

the mean axial velocity, as seen for model *I*. This explains why the difference in rheograms for models *II* and *III* at low shear rates is reflected only in the mean viscosity profiles (Fig. 4b) and not in the mean axial velocity profiles (Fig. 4a). Profiles of the rms velocity fluctuations and Reynolds stress predicted using rheology models *II* and *III* are shown in Fig. 4c and d. They also agree well with each other and deviate only slightly in the wall-region and the buffer-layer. Again, the near-wall, high shear rheology of these two models is similar and results in similar turbulence statistics, despite the differences in predicted viscosity at low shear rates that are typical of the core region.

Additional DNS were run using models *II* and *III* at a lower pressure gradient of $dp/dz = 2.33 \text{ kPa m}^{-1}$. The flow at this pressure gradient is closer to transition. Similar results were observed to the case of 2.72 kPa m^{-1} , with the error in DNS predictions of U_b being -1% with model *II* and -1.77% with model *III*. The corresponding errors obtained using the Wilson–Thomas correlation were 5% and 6.5%.

Summary

These results show that the error introduced in the rheology characterisation by neglecting high shear rate data, can lead to large discrepancies between experiments and predictions using either DNS or the Wilson–Thomas correlation. Discrepancies between the results from DNS and experiments are largely due to incorrect viscosity estimates in the wall-region.

5.2. Effect of rheology model type

As seen in Section 3 and Fig. 2, it is possible to obtain constitutive equations based on different rheology model types (models *III–V*) which agree closely with each other over most of the shear

rate range. These models only deviate from each other significantly at shear rates $\dot{\gamma} < 100 \text{ s}^{-1}$. Based on the results in Section 5.1, we hypothesise that provided high shear rate rheology is used in rheology characterisation, the choice of rheology model type will have a negligible effect on turbulent flow predictions using either DNS or the Wilson–Thomas correlation. In order to test this hypothesis, additional DNS are run using rheology models *IV* (power–law) and *V* (Hallbom) for a pressure gradient $dp/dz = 2.72 \text{ kPa m}^{-1}$.

As seen in Table 3 the bulk velocity predictions using DNS or the Wilson–Thomas correlation with rheology fits *III–V* are close to each other, validating our hypothesis. Similar agreement is seen for the mean axial velocity profile and turbulence statistics where the profiles of models *III–V* overlap each other (Fig. 5). Again the effect of the deviation in the model rheograms is limited to the predicted mean viscosity profiles in the log-layer and the core-region. The reason, also explained in Section 5.1, is that the shear rates are very low in the log-layer and the core-region. Therefore, the shear stress tensor and hence the predictions of the mean axial velocity and the turbulence statistics are affected notably by the deviation in viscosity estimates in the log-layer and the core-region.

5.3. A criterion for the maximum shear rate needed in rheology characterisation

Results presented in Section 5.1 and 5.2 show that high shear rate data is required in rheology characterisation in order to obtain good agreement between the results from experiments and DNS. It has also been shown that it is relevant in obtaining better agreement in the use of empirical correlations, in particular the

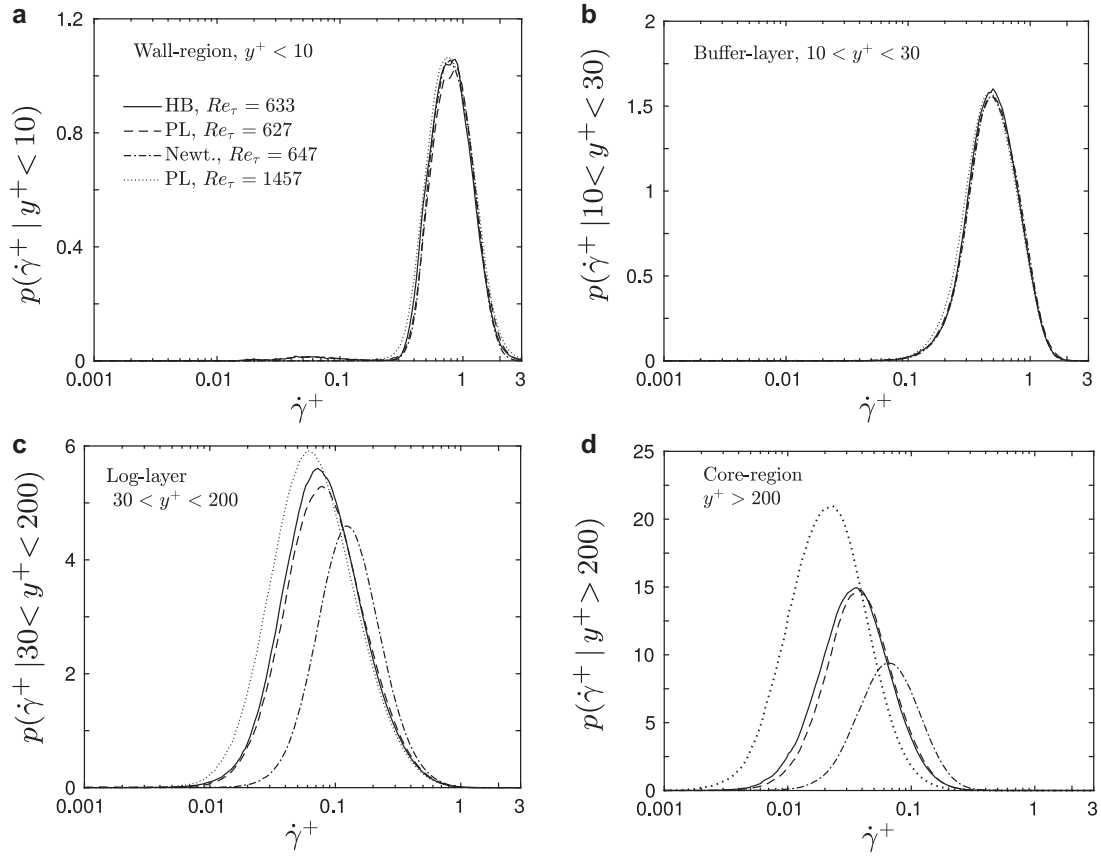


Fig. 7. Profiles of $p(\dot{\gamma}^+|y^+)$ plotted as a function of $\dot{\gamma}^+$ in (a) wall-region (b) buffer-layer (c) log-layer and (d) the core-region for the cases from Fig. 6. Profiles of the probability distribution of different rheology and Re_τ overlap each other in the wall-region and buffer-layer. In wall units, the profiles show rheology and Re_τ dependence only in the log-layer and core-region.

Wilson–Thomas correlation. However, the obvious question is yet to be answered, “How high is high enough?”.

To provide some rigour in developing an answer to this question, instantaneous shear rate distributions in the turbulent flow DNS are analysed using conditional probability densities. This approach identifies the range of shear rates in different parts of the flow volume. The conditional probability density function (pdf) $p(\dot{\gamma}^+|y^+)$ is defined as the probability that the shear rate is equal to $\dot{\gamma}^+$ given that the distance from the wall is given by y^+ . It is normalised such that

$$\int_{y^+=0}^{R^+} \int_{\dot{\gamma}^+=0}^{\infty} p(\dot{\gamma}^+|y^+) d\dot{\gamma}^+ dy^+ = 1. \tag{16}$$

This definition then allows the marginal pdf to be written as a constant

$$p(y^+) = \int_{\dot{\gamma}^+=0}^{\infty} p(\dot{\gamma}^+|y^+) d\dot{\gamma}^+ = 1/R^+ \tag{17}$$

Thus the probability density is weighted by distance (not by area). This is not the only way to normalise the distribution, however it allows more direct comparison with channel flow results by removing the effect of the radial coordinate from the definition.

The full conditional probability density function is calculated in the current simulations for rheology models III and IV in which $Re_\tau \approx 630$ (results for model V, the Hallbom model, are almost indistinguishable and are not shown). The pdf’s are compared with those from our unpublished DNS results of a Newtonian fluid at $Re_\tau = 647$ and a pseudo-plastic fluid modelled with the power-law rheology model at $Re_\tau = 1457$ in Fig. 6. The qualitative picture is very similar for all cases. Decrease in the shear rate magnitude with distance from the wall can be seen clearly in the con-

four plots of $p(\dot{\gamma}^+|y^+)$. The distribution of shear rate is wider near the wall and much narrower (and at lower shear rate) towards the centre of the pipe where the probabilities are also significantly higher. Considering the near-wall shear rates in particular, a large region of non-negligible probability exists for shear rates $\dot{\gamma}^+ > 1$. This suggests that Shook’s criterion, (expressed here as $\dot{\gamma}_{max}^+ = 1$), underestimates the shear rates that bracket the relevant near-wall values, and is not high enough to capture around half of the range that is important.

An alternative way of presenting the same information is to average the conditional pdf’s over ranges of y^+ corresponding to the wall, buffer, log and core regions of the flow. This more clearly highlights similarities and differences between the cases. Averaged pdf’s are presented in Fig. 7. In the wall region, profiles of $p(\dot{\gamma}^+|y^+)$ collapse quite well onto the same profile for different rheologies and at two different Re_τ . The same is observed in the buffer layer, although the profile is different to near-wall, with higher probability and a lower value at which the probability peak occurs. Moving away from the wall, the distributions begin to separate in the log layer and become significantly different in the core. Most notable in the core is that the probability peak for the Newtonian fluid is at a higher shear rate than the two non-Newtonian fluids at similar Re_τ . This behaviour is expected. Although the mean viscosities of the non-Newtonian cases match the Newtonian case at the wall, viscosities are higher in the core for shear-thinning fluids. Consequently shear rates will be lower. The profile for the higher Re_τ power-law case is shifted to lower non-dimensional shear rate and demonstrates that shear rates in the core do not increase linearly with increasing mean wall shear (i.e. increasing Re_τ).

In the near-wall region the profiles of the probability distribution in Fig. 7a (i.e. $p(\dot{\gamma}^+|y^+ < 10)$) spread as high as $\dot{\gamma}^+ \approx 3$ but the value of the probability for $\dot{\gamma}^+ > 2$ is less than 0.1, indicating that the total flow volume with shear rates higher than this is very small. The condition $\dot{\gamma}^+ > 2$ corresponds to $\dot{\gamma} > 5000 \text{ s}^{-1}$ for $Re_\tau \approx 630$. The collapse of these probability profiles in the near-wall are suggestive of a universal near-wall shear rate distribution, although further simulation are required to confirm this collapse for a broader range of the rheologies (in particular with higher yield stress) and for other values of Re_τ . Based on these observations we propose that the maximum shear rate $\dot{\gamma}_{max}^+$ in the rheology characterisation should be 2. This criterion can further be expressed in terms of shear stress using the constitutive equation of rheology model. For the Herschel–Bulkley model it is straight forward to show:

$$\tau/\tau_w = \tau_y/\tau_w + \frac{K}{\rho U_\tau^{2(1-n)} \nu_w^n} (\dot{\gamma}^+)^n \quad (18)$$

With $\dot{\gamma}_{max}^+ = 2$ this equation can be rewritten to give τ_{max} as

$$\tau_{max}/\tau_w = 2^n - (2^n - 1)\tau_y/\tau_w \quad (19)$$

For shear thinning Herschel–Bulkley fluids, Eq. 19 is a maximum when n approaches one and the yield stress approaches zero, i.e. the maximum value it can take is 2. Hence, in terms of all shear thinning Herschel–Bulkley fluids, using rheology characterisation at shear stresses given by $\tau_{max} = 2\tau_w$ will provide a margin of safety in the measurements.

6. Conclusions

This study shows that choosing an appropriate shear rate range in rheology characterisation is crucial in obtaining good turbulent flow predictions using DNS and influences in a positive way the results obtained from the Wilson–Thomas correlation. Standard methods of determining rheology model parameters such as using the laminar pipe flow curve or from low shear rate rheograms, can result in large error in turbulent flow predictions. Fundamentally, this study shows the familiar dangers associated with extrapolation of data. It serves as a reminder to practitioners that extrapolating rheology outside the range where it was measured can result in unreliable predictions using DNS or empirical correlation.

Results obtained with three simple rheology models namely the power–law, Herschel–Bulkley and the Hallbom models, which are commonly used in applications, show that if an appropriate range of shear rate is considered in the rheology characterisation, the model type has a little effect on turbulent flow predictions. This means that using a more complex rheology model or using a piece-wise fit to the rheology data to improve the accuracy of the model at lower shear rates will not have a significant effect on the turbulent flow predictions using DNS or the Wilson–Thomas correlation. The effect of errors introduced at low shear rates due to poor rheology measurements or poor fitting were found to be limited to the mean viscosity predictions in the log-layer and core-region. They do not affect the profiles of the mean axial velocity or the turbulence statistics to any notable extent.

In the near-wall region and the buffer-layer where shear rates are highest, the conditional probability distributions of non-dimensionalised, instantaneous shear rates are found to be essentially independent of rheology and Reynolds number. Based on this observation we propose that the maximum shear rate in rheology characterisation should be at least twice the mean wall shear rate. When expressed in terms of shear stress, Eq. 19 provides the same criteria, although using the simpler value of twice the mean wall shear stress will provide a margin of safety.

The comparison between DNS and experiments presented in the current study is based entirely on bulk velocity because velocity profiles and turbulence statistics could not be measured in

the current experimental facility. However, the previous comparisons [14] to experimental mean flow profiles showed the DNS was able to predict the correct form (but not magnitude) of the profiles. When coupled to a demonstration of the correct integrated velocity, demonstrated in this paper, the results collectively suggest the complete picture is likely to be correct. However, only consistent measurement will prove this conclusively.

We note that Peixinho *et al.* [23] carried out pipe flow measurements in the turbulent regime using a 0.2 wt% Carbopol solution and measured the rheology at high shear rates. However, the Carbopol fluid used in their study was acknowledged to show viscoelastic effects at Reynolds numbers they considered i.e. the fluid showed a partial recovery when the applied shear stress is removed. Therefore, their experimental measurements could not be used in the current study for validation purposes as visco-elastic effects are likely to be influencing the measurements.

As a final point, although we advocate the use of high shear rate rheology in rheological characterisation, in practice it could be very difficult to measure such rheology in fine particle mineral suspensions such as the mining and waste slurries that have motivated this study. In these fluids centrifugal effects in most rheometric methodologies will tend to separate the solids—even for very small particles. Accurate rheology measurement of these fluids at high shear rates therefore remains an open problem.

Acknowledgements

This research was supported via AMIRA project P1087 funded through AMIRA International by; Anglo Operations, Freeport McMoran, Gold Fields, Total E&P Canada, Newmont, Shell Canada Energy, BASF, Nalco and Outotec. The authors thank them for their support.

Computations in this study were carried out using the resources provided by the Pawsey Supercomputing Centre with funding from the Australian Government and the Government of Western Australia via merit allocation scheme grant number D77. We gratefully acknowledge the resources and their support.

References

- [1] A.B. Metzner, J.C. Reed, Flow of non-newtonian fluids – correlations for laminar, transition and turbulent flow regimes, *A. I. Ch. E. J.* 1 (1955) 434–444.
- [2] D.W. Dodge, A.B. Metzner, Turbulent flow of non-Newtonian systems, *A. I. Ch. E. J.* 5 (1959) 189–204.
- [3] R.M. Clapp, Turbulent heat transfer in pseudoplastic non-Newtonian fluids, in: *International Development in Heat Transfer*, 1961, pp. 652–661. A. S. M. E., Part 111, Sec. A.
- [4] D.C. Bogue, A.B. Metzner, Velocity profiles in turbulent pipe flow. Newtonian and non-Newtonian fluids, *Ind. Eng. Chem. Fundam.* 2 (2) (1963) 143–149.
- [5] J. Park, T. Mannheimer, T. Grimley, Pipe flow measurements of transparent non-Newtonian slurry, *J. Fluids Eng.* 111 (3) (1989) 331–336.
- [6] F.T. Pinho, J.H. Whitelaw, Flow of non-Newtonian fluids in a pipe, *J. non-Newtonian Fluid Mech.* 34 (1990) 129–144.
- [7] R. Chhabra, J. Richardson, *Non-Newtonian Flow and Applied Rheology*, second ed., Elsevier, 2008.
- [8] D.J. Hallbom, Pipe flow of homogeneous slurry, Citeseer, 2008 Ph.D. thesis.
- [9] W.H. Herschel, R. Bulkley, Measurement of consistency as applied to rubber-benzene solutions, *Proc. Annu. Meet. Am. Soc. Test Mater.* 26 (1926) 621–633.
- [10] D. Hallbom, B. Klein, A physical model for yield plastic fluids, *Particul. Sci. Technol.* 27 (1) (2009) 1–15.
- [11] R. de Kretser, P.J. Scales, D.V. Boger, Improving clay-based tailings disposal: case study on coal tailings, *AIChE J.* 43 (7) (1997) 1894–1903.
- [12] N. Heywood, D.-H. Cheng, Comparison of methods for predicting head loss in turbulent pipe flow of non-Newtonian fluids, *Trans. Inst. of Meas. Control* 6 (1) (1984) 33–45.
- [13] E.V.d. Heever, A. Sutherland, R. Haldenwang, Influence of the rheological model used in pipe-flow prediction techniques for homogeneous non-newtonian fluids, *J. Hydraulic Eng.* 140 (12) (2014) 04014059.
- [14] M. Rudman, H.M. Blackburn, L.J.W. Graham, L. Pullum, Turbulent pipe flow of shear-thinning fluids, *J. Non-Newt. Fluid Mech.* 118 (1) (2004) 33–48.
- [15] M. Rudman, H.M. Blackburn, Direct numerical simulation of turbulent non-Newtonian flow using a spectral element method, *Appl. Math. Mod.* 30 (2006) 1229–1248.

- [16] S. Guillou, R. Makhloufi, Effect of a shear-thickening rheological behaviour on the friction coefficient in a plane channel flow: a study by Direct Numerical Simulation, *J. Non-Newt. Fluid Mech.* 144 (2007) 73–86.
- [17] H.M. Blackburn, S.J. Sherwin, Formulation of a galerkin spectral element–fourier method for three-dimensional incompressible flows in cylindrical geometries, *J. Comput. Phys.* 197 (2) (2004) 759–778.
- [18] K.C. Wilson, A.D. Thomas, A new analysis of the turbulent flow of non-newtonian fluids, *Can. J. Chem. Eng.* 63 (4) (1985) 539–546.
- [19] C. Shook, M. Roco, *Slurry Flow*, Butterworth-Heinemann, 1991.
- [20] G.I. Taylor, Stability of a viscous liquid contained between two rotating cylinders, *Philos. Trans. R. Soc. Lond. series a* 223 (1923) 289–343. Containing Papers of a Mathematical or Physical Character
- [21] W.C. MacSporran, Direct numerical evaluation of shear rates in concentric cylinder viscometry, *J. Rheology* (1978-present) 30 (1) (1986) 125–132.
- [22] K. Walters, *Rheometry/K.Walters*, Vol. 1, Chapman and Hall, New York, London, 1975. distributed by Halstead Press
- [23] J. Peixinho, C. Nouar, C. Desaubry, B. Thron, Laminar transitional and turbulent flow of yield stress fluid in a pipe, *J. Non-Newtonian Fluid Mech.* 128 (23) (2005) 172–184.
- [24] U. Piomelli, Large-eddy simulations: where we stand, in: C. Liu, Z. Liu (Eds.), *Advances in DNS/LES, AFOSR*, Greyden Press, 1997, pp. 93–104. Louisiana
- [25] E.J. Garcia, J.F. Steffe, Comparison of friction factor equations for non-newtonian fluids in pipe flow, *J. Food Process Eng.* 9 (2) (1986) 93–120.
- [26] J. Hartnett, M. Kostic, Turbulent friction factor correlations for power law fluids in circular and non-circular channels, *Int. Commun. in Heat Mass Transf.* 17 (1) (1990) 59–65.
- [27] P. Gao, J.-J. Zhang, New assessment of friction factor correlations for power law fluids in turbulent pipe flow: a statistical approach, *J. Cent. S. Univ. Technol.* 14 (2007) 77–81.